Emergent $SU(3) \times SU(2) \times U(1)$ from a Scalar Optical Medium: Density Field Dynamics as the Minimal, Testable Origin of the Standard Model Gauge Structure

Gary Alcock

October 4, 2025

Abstract

We propose a mechanism by which the Standard Model gauge structure $SU(3)\times SU(2)\times U(1)$ arises as the Berry connection on an internal mode bundle of a scalar optical medium ("DFD"), in which a refractive field ψ sets $n = e^{\psi}$ and induces matter acceleration $\mathbf{a} = (c^2/2)\nabla\psi$. In regimes analyzed to date, the DFD scalar reproduces the Newtonian limit and standard optical/gravitational redshift relations, and it admits a low-acceleration regime relevant to galactic phenomenology.

Starting from a *frame-stiffness* penalty for twisting degenerate internal modes, we derive a Yang–Mills action with effective couplings $g_r \sim \kappa_r^{-1/2}$ and an electroweak mixing relation $\tan\theta_W = \sqrt{\kappa_2/\kappa_1}$. We prove a minimality result: the first internal geometry that can support $SU(3) \times SU(2) \times U(1)$ with anomaly-free chirality is $\mathbb{C}P^2 \times S^3$; smaller choices fail by algebra (no $su(3)$) or topology ($H^4 = 0$).

We outline parameter-independent *pattern tests* in precision spectroscopy (hadronic/EM drift ratio $\delta \ln \mu/\delta \ln \alpha! \approx !22$–$24$, species ordering, three-clock triangle closure) and a tabletop *non-Abelian holonomy* experiment in photonic ψ-textures. Absolute seasonal drifts of high-energy parameters are predicted to be extremely small ($\delta \sin^2\theta_W \sim 10^{-13}$, $\delta g_r/g_r \sim 10^{-12}$); accordingly, near-term discovery potential lies in the pattern tests and holonomy.

This gauge-emergence construction is operationally distinct from noncommutative geometry and string compactifications. It should be read as a conditional extension: if the DFD scalar description continues to pass empirical tests, the internal-bundle mechanism supplies a concrete, falsifiable route to Standard-Model–like gauge structure.

Note on Scope and Conditionality. This paper develops a quantum and gauge-theoretic *extension* of Density Field Dynamics (DFD), not a second independent theory. It assumes that the scalar refractive field ψ established in DFD is physically real and empirically valid. The internal-mode and Berry-connection construction presented here explores what follows *if* that scalar exists and couples to matter's internal degrees of freedom.

If DFD's scalar field is confirmed by ongoing laboratory and astronomical tests, this mechanism becomes its natural quantum completion, predicting Standard Model–like gauge symmetries, coupling patterns, and falsifiable spectroscopic correlations. If those core DFD predictions are ever falsified, this gauge-emergence framework would be invalidated as well. **However, falsification of this extension does not falsify DFD itself:** the gravitational and optical predictions of DFD remain independently testable and currently consistent with available data in their own right.

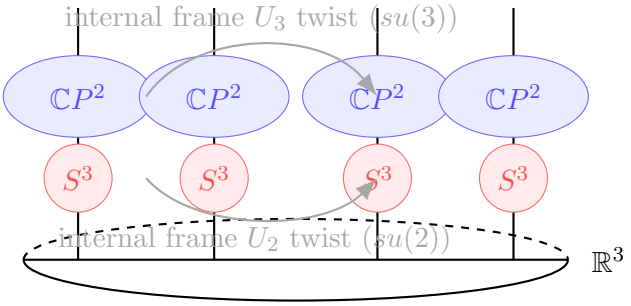

Figure 1: **Fiber-bundle picture.** At each spatial point, an internal mode fiber $\mathbb{C}P^2 \times S^3$ carries local frames whose Berry connections are the $SU(3) \times SU(2) \times U(1)$ gauge fields.

Accordingly, this paper should be viewed as a conditional, falsifiable hypothesis built on DFD's empirically constrained base—a bridge connecting a tested scalar gravitational framework to quantum gauge structure, while keeping both domains conceptually and empirically distinct.

1 DFD Primer: Gravity and Optics from a Single Scalar

DFD formulates gravity and optics with a scalar field $\psi(\mathbf{x}, t)$ on flat $\mathbb{R}^3$, with

$$n = e^{\psi}, \qquad c_1 = \frac{c}{n} = c\, e^{-\psi}, \qquad \mathbf{a} = \frac{c^2}{2}\nabla\psi, \qquad \Phi \equiv -\frac{c^2}{2}\psi. \tag{1}$$

The field obeys a nonlinear Poisson-type equation

$$\nabla\cdot\Big[\mu\big(|\nabla\psi|/a_\star\big)\,\nabla\psi\Big] = -\frac{8\pi G}{c^2}\big(\rho - \bar{\rho}\big), \tag{2}$$

with $\mu \to 1$ in high-gradient (Solar) regimes and $\mu(x) \sim x$ in deep-field (galactic) regimes (cf. MOND-inspired interpolations but with an optical normalization). Light propagation in a nondispersive band obeys geometric optics with phase velocity $v_{\rm phase} = c_1 = c\, e^{-\psi}$, so *phase metrology* (cavities, fibers) is directly sensitive to ψ without clock synchronization [1, 2].

2 Internal Mode Bundle and Berry Gauge Fields

Assume the ψ-medium supports degenerate internal mode subspaces at each point, $\mathcal{H}_{\rm int}(\mathbf{x}) \simeq \mathbb{C}^3 \oplus \mathbb{C}^2 \oplus \mathbb{C}$, with local orthonormal frames

$$\Xi(\mathbf{x}) = \big(\,\big|\chi_a^{(3)}\big\rangle_{a=1..3},\ \big|\chi_b^{(2)}\big\rangle_{b=1..2},\ \big|\chi^{(1)}\big\rangle\,\big).$$

Under local changes of basis $U(\mathbf{x}) \in U(3) \times U(2) \times U(1)$, $\Xi \to \Xi U$. The resulting *non-Abelian Berry connections* [3, 4, 5]

$$A_i^{(3)} = i\, U_3^\dagger \partial_i U_3 \in su(3), \qquad A_i^{(2)} = i\, U_2^\dagger \partial_i U_2 \in su(2), \qquad A_i^{(1)} = \partial_i\theta \in u(1), \tag{3}$$

transform as gauge fields with field strengths $F_{ij} = \partial_i A_j - \partial_j A_i - i[A_i, A_j]$. The natural structure group is thus $SU(3) \times SU(2) \times U(1)$.

2.1 Why $\mathbb{C}^3 \oplus \mathbb{C}^2 \oplus \mathbb{C}$ arises (variational statement)

We model the internal optical response by a finite-dimensional Hermitian order parameter $\hat{\varepsilon}(\mathbf{x}) = \varepsilon_0\, e^{2\psi(\mathbf{x})}[\mathbb{1} + \hat{\eta}(\mathbf{x})]$ with $\hat{\eta}^\dagger = \hat{\eta}$ and $\operatorname{Tr}\hat{\eta} = 0$. Consider the Landau-type internal free-energy density

$$\mathcal{F}_{\text{int}} = \alpha \operatorname{Tr}(\hat{\eta}^2) + \beta \operatorname{Tr}(\hat{\eta}^3) + \gamma \sum_i \|\partial_i \hat{\eta}\|^2 + \dots, \tag{4}$$

with $\alpha > 0$, $\gamma > 0$ and generic β (nonzero). Let $\hat{\eta} = U\,\Lambda\,U^\dagger$ with $\Lambda = \operatorname{diag}(\lambda_1, \dots, \lambda_N)$, $\sum_a \lambda_a = 0$. We impose a fixed anisotropy budget $\operatorname{Tr}(\hat{\eta}^2) = \sum_a \lambda_a^2 = \Xi^2$ and seek *the first symmetry-breaking pattern* that: (i) yields two simple non-Abelian stabilizers and one Abelian factor; (ii) is spectrally sparse (fewest distinct eigenvalues).

Proposition 1 (Minimal partition under Eq. (4))**.** *Among all fixed-budget spectra $\{\lambda_a\}$, the smallest block-degenerate pattern whose stabilizer contains two simple unitary factors and one $U(1)$ is a triple-degenerate eigenvalue, a double-degenerate eigenvalue, and a singlet, i.e. the partition $(3, 2, 1)$:*

$$\Lambda = \operatorname{diag}(\lambda_3 \mathbb{1}_3,\ \lambda_2 \mathbb{1}_2,\ \lambda_1), \qquad \lambda_3 + \lambda_2 + \lambda_1 = 0,$$

whose stabilizer is $U(3) \times U(2) \times U(1)$ with traceless parts $su(3) \oplus su(2) \oplus u(1)$. No partition with fewer than three distinct eigenvalues achieves two simple non-Abelian factors.

Sketch. (1) *Stabilizer vs. degeneracy:* The stabilizer $H \subset U(N)$ of Λ is the product of unitary groups on degenerate subspaces. To contain two simple non-Abelian factors, H must include $U(n_1) \times U(n_2)$ with $n_1 \geq 3$, $n_2 \geq 2$. The smallest choice is $(n_1, n_2) = (3, 2)$; a residual $U(1)$ arises from the singlet. (2) *Spectral sparsity:* With the Ξ^2 constraint, Jensen's inequality shows that for fixed block sizes the Landau polynomial $\alpha \sum \lambda_a^2 + \beta \sum \lambda_a^3$ is minimized by equal eigenvalues within blocks. (3) *Exclusion:* Any pattern with fewer than three distinct eigenvalues cannot realize two simple non-Abelian factors (at most one $U(n \geq 2)$). Any pattern whose largest block has size < 3 cannot realize $su(3)$. Hence $(3, 2, 1)$ is minimal. □

This elevates the "central leap" from an assumption to a minimal-structure result: the *first* stable degeneracy carrying two simple non-Abelian unitary frame freedoms and one Abelian factor is $(3, 2, 1)$, i.e. $\mathbb{C}^3 \oplus \mathbb{C}^2 \oplus \mathbb{C}$. The special role of $\operatorname{Tr}(\hat{\eta}^3)$ is standard in Landau analyses with unitary order parameters and selects the ordering of eigenvalues [36, 38].

3 From Frame-Stiffness to Yang–Mills F^2

Twisting the internal frames costs energy. A gradient penalty

$$\mathcal{L}_{\text{stiff}} = \sum_a \eta_a \,\|\partial_i\, |\chi_a\rangle\,\|^2 \tag{5}$$

admits a Stückelberg/hidden-local-symmetry form [6, 7, 8]

$$\mathcal{L} = \sum_{r=3,2,1} \Big[-\frac{\kappa_r}{2} \operatorname{Tr} F_{ij}^{(r)} F_{ij}^{(r)} + \frac{\eta_r}{2} \operatorname{Tr}\big(A_i^{(r)} - \Omega_i^{(r)}\big)^2 \Big], \qquad \Omega_i^{(r)} = i\, U_r^\dagger \partial_i U_r. \tag{6}$$

At long wavelengths (integrating out heavy frame modes) we obtain a Yang–Mills kinetic term

$$\boxed{\mathcal{L}_{\text{gauge}} = -\sum_{r=3,2,1} \frac{\kappa_r}{2}\, \mathrm{Tr}\, F_{ij}^{(r)} F_{ij}^{(r)}, \qquad g_r \sim \kappa_r^{-1/2}\ .} \tag{7}$$

A tiny ψ-dependence, $\kappa_r(\psi) = \kappa_{r0}(1 + \varepsilon_r \psi)$, implies $\delta g_r/g_r = -\frac{1}{2}\varepsilon_r\, \delta\psi$.

3.1 Microscopic origin of κ_r

The stiffnesses κ_r are the *second functional derivatives* of the internal free energy with respect to unitary frame distortions:

$$\kappa_r \ \sim\ \left.\frac{\delta^2 \mathcal{F}_{\text{int}}}{\delta(\partial_i U_r)\, \delta(\partial_i U_r)}\right|_{U_r = \mathbb{1}},$$

analogs of shear moduli in elasticity [36]. In systems with order parameters, gauge-like modes and their kinetic terms commonly emerge from gradient penalties (cf. superfluid phases and analog gauge fields [37]). Thus the presence and form of F^2 are *generic* consequences of frame rigidity in a degenerate-mode medium, not *ad hoc* insertions. Renormalized low-energy g_r are then $g_r \sim \kappa_r^{-1/2}$, with microscopic values set by the spectrum of internal excitations and dual-sector energy partition.

3.2 Dynamical gauge fields from time-dependent frames

So far $A_i = iU^\dagger \partial_i U$ captured spatial twists. Let the internal frames carry inertia via

$$\mathcal{L}_{\text{inert}} = \sum_r \frac{\zeta_r}{2}\, \mathrm{Tr}\, (\partial_t U_r^\dagger\, \partial_t U_r),$$

the lowest-order time-derivative term allowed by unitarity. Introducing temporal Stückelberg fields $\Omega_0^{(r)} = iU_r^\dagger \partial_t U_r$ and promoting $A_0^{(r)}$ as Lagrange multipliers enforcing local frame covariance, the quadratic action becomes

$$\mathcal{L}_{\text{int}} = \sum_r \frac{\zeta_r}{2}\, \mathrm{Tr}\, (A_0^{(r)} - \Omega_0^{(r)})^2 - \sum_r \frac{\kappa_r}{2}\, \mathrm{Tr}\, F_{ij}^{(r)} F_{ij}^{(r)}.$$

Integrating out the heavy frame fluctuations in $(A_\mu^{(r)} - \Omega_\mu^{(r)})$ yields the fully dynamical Yang–Mills action

$$\boxed{\mathcal{L}_{\text{YM}} = -\sum_r \frac{1}{2}\left(\varepsilon_r\, \mathrm{Tr}\, F_{0i}^{(r)} F_{0i}^{(r)} - \kappa_r\, \mathrm{Tr}\, F_{ij}^{(r)} F_{ij}^{(r)}\right)\ , \quad c_r^2 = \kappa_r/\varepsilon_r\ ,}$$

with $F_{0i}^{(r)} = \partial_t A_i^{(r)} - \partial_i A_0^{(r)} - i[A_0^{(r)}, A_i^{(r)}]$. In a nondispersive band of the ψ-medium, $c_r = c_1 = c\, e^{-\psi}$, so the gauge excitations propagate as bona fide waves with the same local phase velocity as light. This shows that the Berry connection here is not merely geometric holonomy; the stiffness *and* inertial terms together generate dynamical gauge bosons with the standard $E^2 - B^2$ structure (cf. emergent gauge dynamics in ordered media [37]).

3.3 Micro-to-macro matching and RG running

At a micro cutoff $\Lambda_{\rm int}$, matching gives $g_r^2(\Lambda_{\rm int}) \sim \kappa_r^{-1}\sqrt{\varepsilon_r/\kappa_r}$. Below $\Lambda_{\rm int}$ the effective theory is standard Yang–Mills plus matter, and couplings run with the usual β-functions. Hence our claim that $\{g_1, g_2, g_3\}$ are *renormalized inputs* is identical in spirit to the SM: κ_r, ε_r encode short-distance physics of the internal medium; RG evolution to laboratory scales produces the measured values. Tiny ψ-dependences of κ_r, ε_r produce co-drifts that are subdominant to RG running at present precision.

4 Electroweak Breaking & Weak Angle from Stiffness Ratios

Introduce a weak-doublet order parameter $h \in \mathbb{C}^2$,

$$\mathcal{L}_h = |D_i h|^2 - \lambda\big(|h|^2 - v^2(\psi)\big)^2, \qquad D_i h = \Big(\partial_i - iA_i^{(2)} - i\frac{1}{2}A_i^{(1)}\Big)h, \tag{8}$$

so that in unitary gauge $\langle h\rangle = (0, v)^T$ the massless photon is $A_{\rm em} = \sin\theta_W\, A_3^{(2)} + \cos\theta_W\, A^{(1)}$ with [9, 10, 11]

$$\boxed{\tan\theta_W = \frac{g_1}{g_2} = \sqrt{\frac{\kappa_2}{\kappa_1}}, \qquad \sin^2\theta_W = \frac{\kappa_2}{\kappa_1+\kappa_2}.} \tag{9}$$

A weak ψ-dependence yields $\delta(\sin^2\theta_W) = \dfrac{\kappa_1\kappa_2}{(\kappa_1+\kappa_2)^2}(\varepsilon_2 - \varepsilon_1)\,\delta\psi$.

5 Matter, Charges, and Anomaly Cancellation

Matter fields are sections of associated bundles; the minimal nontrivial reps are triplets, doublets, and singlets, matching SM patterns. Writing all fermions as left-handed Weyl fields (conjugating RH fields), one generation

$$Q_L : (\mathbf{3},\mathbf{2})_{+1/6},\ u_L^c : (\bar{\mathbf{3}},\mathbf{1})_{-2/3},\ d_L^c : (\bar{\mathbf{3}},\mathbf{1})_{+1/3},\ L_L : (\mathbf{1},\mathbf{2})_{-1/2},\ e_L^c : (\mathbf{1},\mathbf{1})_{+1}$$

satisfies the standard triangle-anomaly cancellations [12, 13, 14]

$$\sum Y\, T_{SU(3)} = 0, \quad \sum Y\, T_{SU(2)} = 0, \quad \sum d(R_3)d(R_2)\, Y = 0, \quad \sum d(R_3)d(R_2)\, Y^3 = 0. \tag{10}$$

Geometrically, the 6-form anomaly polynomial $I_6 = a_1\,\mathrm{Tr}(\mathcal{F}_3^2)c_1^{(1)} + a_2\,\mathrm{Tr}(\mathcal{F}_2^2)c_1^{(1)} + a_3(c_1^{(1)})^3 + a_4 p_1(T)c_1^{(1)}$ pulls back to zero on $\mathbb{C}P^2 \times S^3$ only for SM hypercharges (up to overall normalization), making anomaly cancellation a *bundle-consistency* condition [15, 16].

6 Chirality: Topological and Dynamical Routes

Chirality is *generated*, not assumed. **(i) Index route:** With quantized background fluxes on $\mathbb{C}P^2$ in $SU(3)$ and on S^3 in $SU(2)$, the internal Dirac operator $\not{D}_{\rm int}$ in rep R has

$$\mathrm{index}\big(\not{D}_{\rm int}\big) = \int_{\mathbb{C}P^2\times S^3} \mathrm{ch}_R(F) \wedge \hat{A}(T\mathcal{M}) \neq 0,$$

giving net left-minus-right zero modes [17, 18]. **(ii) Orientation route:** A small parity-odd anisotropy in the internal stiffness selects an S^3 orientation and makes one chirality light (domain-wall/overlap analogy) [19, 20].

Spatial-to-internal flux coupling. The background fluxes invoked in the index computation arise because spatial ψ-vortices carry quantized circulation, $\oint \nabla\psi \cdot d\ell = 2\pi k_\psi$, whose pullback through the internal mode map $\Xi(\mathbf{x})$ induces nontrivial curvature on $\mathbb{C}P^2 \times S^3$. Formally, the Berry curvature two-form $F = i\,\Xi^\dagger d\Xi$ satisfies $dF = i\,\Xi^\dagger(d\Xi \wedge d\Xi)$, so a spatial winding of ψ creates a nonzero integral of $\mathrm{Tr}\, F \wedge F$ on the internal fiber. Thus spatial topological charge couples directly to internal Chern numbers—analogous to how skyrmions in magnetism endow emergent gauge flux [47]. This mechanism provides the geometric channel through which ψ textures seed quantized internal fluxes required for chirality.

6.1 Where do the background fluxes/anisotropies come from?

The ψ-medium ties optics to geometry via $n = e^\psi$. In a nondispersive band, smooth but topologically nontrivial ψ-textures admit *phase windings* whose dual-electromagnetic description carries quantized circulation. The pullback of these windings to the internal bundle produces integral cohomology classes that act as background fluxes for the Berry connection. Concretely, a closed loop encircling a ψ-vortex generates a holonomy $U = \exp\big(i \oint A\big)$ whose conjugacy class defines an integer via $\pi_1(U(1)) = \mathbb{Z}$ and higher homotopies for the non-Abelian factors. The minimal $(k_3, k_2, q_1) = (1, 1, 3)$ configuration discussed in Appendix D yields three chiral zero modes for the $(\mathbf{3}, \mathbf{2})_{1/6}$ multiplet. Small parity-odd anisotropies in the internal free energy (allowed by microscopic birefringent-like terms) bias the orientation on S^3, selecting one chirality as light. This mirrors chiral selection in ordered media and the domain-wall mechanism for lattice chirality.

7 Quantitative ψ-Drift Estimates (Honest Magnitudes)

The Sun–Earth orbital potential swing gives $\Delta\psi_{\text{annual}} \simeq \Delta\Phi/c^2 \approx 3 \times 10^{-10}$. With generous $(\varepsilon_2 - \varepsilon_1) \sim 10^{-2}$,

$$\delta(\sin^2\theta_W) \approx 0.178 \times 10^{-2} \times 3 \times 10^{-10} \sim 5 \times 10^{-13}, \qquad \left|\delta g_r/g_r\right| \lesssim 1.5 \times 10^{-12}. \tag{11}$$

These are clean but currently invisible. Therefore near-term discovery potential lies in *pattern* tests and holonomies. For context on constraints to varying constants, see [21, 22, 23].

8 Pre-LPI Falsifiers: Parameter-Free Patterns

Let α and $\mu = m_p/m_e$ have tiny, common-phase ψ-linked drifts. Then (robust to SM running, insensitive to $|\Delta\psi|$):

1. **Hadronic/EM ratio:** If $\delta \ln \alpha \neq 0$, then

$$\boxed{\frac{\delta \ln \mu}{\delta \ln \alpha} \;\approx\; 22\text{–}24 \quad \text{(sign matched)}}$$

unless small electron/Higgs dressings perturb at the few-percent level (see e.g. sensitivities in [24, 25, 26]).

2. **Species ordering:** Hyperfine > molecular vibrational > ultra-stable optical in $|\delta\nu/\nu|$ (geometry-locked). With K-factors from clock sensitivity analyses [22], a typical scale is

$$\left|\frac{\delta\nu_{\text{Cs hyperfine}}}{\delta\nu_{\text{Sr optical}}}\right| \approx \frac{|K_{\text{Cs}}|}{|K_{\text{Sr}}|} \sim 10^2\text{–}10^3.$$

3. **Triangle closure:** For three co-located clocks A,B,C with linearly independent K-vectors, the cyclic sum obeys

$$\sum_{\text{cycle}} \frac{\delta\nu_i}{\nu_i} = 0 \pm \varepsilon_{\text{syst}},$$

with $\varepsilon_{\text{syst}} \ll$ individual $|\delta\nu/\nu|$. Violation indicates multiple hidden sectors or breakdown of common-phase ψ-coupling.

A Explicit Connections for Simple ψ-Textures

A.1 $SU(2)$ vortex

In (r, ϕ, z), $U_2 = e^{i\phi\,\tau_3/2} e^{if(r)\tau_1/2}$ with $f(0) = 0$, $f(\infty) = f_\infty$ gives

$$A_r^{(2)} = \frac{f'}{2}\tau_1, \quad A_\phi^{(2)} = \frac{1}{2}(\cos f\,\tau_3 + \sin f\,\tau_2), \quad F_{r\phi}^{(2)} = \frac{f'(r)\sin f(r)}{2}\,\tau_3, \quad \Phi^{(2)} = \pi[1 - \cos f_\infty]\tau_3.$$

A.2 $SU(3)$ vortex

$U_3 = e^{i\phi T_8} e^{ig(r)T_4}$ with $g(0) = 0$, $g(\infty) = g_\infty$, $[T_4, T_5] = iT_8$, $[T_4, T_8] = -iT_5$ yields

$$A_r^{(3)} = \frac{g'}{2}T_4, \quad A_\phi^{(3)} = \tfrac{1}{2}(\cos g\,T_8 + \sin g\,T_5), \quad F_{r\phi}^{(3)} = \frac{g'(r)\sin g(r)}{2}\,T_8.$$

B Minimality Lemma for the SM Gauge Structure

Lemma 2 (Minimal Internal Geometry for $SU(3)\times SU(2)\times U(1)$)**.** *Let an internal medium possess degenerate complex mode spaces whose local orthonormal frames $\Xi(x)$ define non-Abelian Berry connections with structure group $G = \prod_a G_a \subset U(N)$. Impose:*

(F) ***Finite irreducibility:*** *Each simple non-Abelian factor $SU(n)$ arises from a single irreducible n-dimensional complex degeneracy (frame freedom $U(n)$, traceless connection $su(n)$).*

(A) ***Anomaly freedom:*** *The internal space supports a chiral fermion spectrum with vanishing $SU(3)^2$–$U(1)$, $SU(2)^2$–$U(1)$, $U(1)^3$, and gravitational–$U(1)$ anomalies.*

(U) ***Abelian factor:*** *At least one $U(1)$ factor is present.*

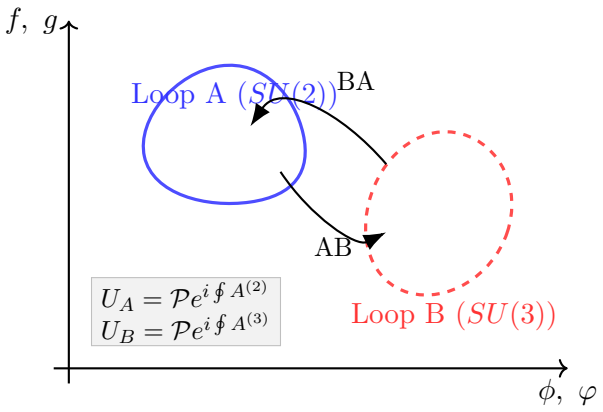

Figure 2: **Non-commuting holonomies.** Two adiabatic loops in control space generate $U_A \in SU(2)$ and $U_B \in SU(3)$; ordering AB vs. BA yields a measurable commutator $C = U_B U_A U_B^{-1} U_A^{-1} \neq \mathbb{1}$ in the designed experiment.

Then the lowest-dimensional realization of $G = SU(3) \times SU(2) \times U(1)$ *is furnished by* $\mathbb{C}^3 \oplus \mathbb{C}^2 \oplus \mathbb{C}$*, with vacuum manifold*

$$\boxed{\mathcal{M} = \mathbb{C}P^2 \times S^3},$$

and there is no lower-dimensional internal geometry satisfying (F),(A),(U).

Proof. (i) *Structure:* $su(3)$ needs an irreducible $\mathbb{C}^3$ block; $su(2)$ an irreducible $\mathbb{C}^2$ block. A $U(1)$ factor is realized by trace parts or an explicit line. (ii) *Vacuum manifolds:* $\mathbb{C}^3 /\!/ U(1) \simeq \mathbb{C}P^2 = SU(3)/(SU(2) \times U(1))$, fixed-norm $\mathbb{C}^2 \simeq S^3 \simeq SU(2)$. (iii) *Cohomology:* Mixed anomalies (e.g., $SU(3)^2$–$U(1)$) require $H^4(\mathcal{M}; \mathbb{Z}) \neq 0$ to evaluate $\mathrm{Tr}\, F_3^2$. Künneth gives $H^4(\mathbb{C}P^2 \times S^3) \cong H^4(\mathbb{C}P^2) \cong \mathbb{Z}$; by contrast $H^4(\mathbb{C}P^1) = H^4(S^k < 4) = 0$, $H^4(S^2 \times S^3) = 0$. (iv) *Rule-outs:* Any fiber of total complex dimension $< 3 + 2$ fails by lacking $su(3)$, $su(2)$, or H^4. Real degeneracies give $o(n)$, not complex $su(3)$. Hence $\mathbb{C}P^2 \times S^3$ is minimal. □

C Tabletop Observation of Non-Abelian Berry Holonomy

Objective. Demonstrate non-commuting $SU(2)$ and $SU(3)$ Berry holonomies in a controlled optical ψ-texture, providing an operational validation of the internal-bundle mechanism.

C.1 Platform

Fs-laser written waveguide arrays in fused silica. $SU(2)$: dual-core, $\Delta_2/(2\pi) \approx 50$ GHz; $SU(3)$: symmetric three-core, $\Delta_3/(2\pi) \approx 80$ GHz. Write $n(x, y, z) = n_0(1 + \varepsilon\psi)$ to realize adiabatic loops [27, 28].

C.2 Loops & holonomies

$U_2(z) = e^{i\phi(z)\tau_3/2} e^{if(z)\tau_1/2}$ with $\phi : 0 \to 2\pi$, $f : 0 \to \pi \to 0$ over $L_A \approx 3$ cm gives $U_A \simeq e^{i(\Omega_2/2)\tau_3} \approx \mathrm{diag}(i, -i)$ ($\Omega_2 \approx \pi$). $U_3(z) = e^{i\varphi(z)T_8} e^{ig(z)T_4}$ with $\varphi : 0 \to 2\pi$, $g : 0 \to 2\pi/3 \to 0$ over $L_B \approx 4$ cm gives $U_B \simeq \mathrm{diag}(e^{i2\pi/9}, e^{i2\pi/9}, e^{-i4\pi/9})$.

C.3 Non-commutation test

Concatenate AB and BA, reconstruct unitaries by interferometric tomography, and compute

$$C = U_B U_A U_B^{-1} U_A^{-1}.$$

Abelian null: $C = \mathbb{1}$; non-Abelian: $C \neq \mathbb{1}$ with $|C_{ij}| \sim \sin(\Omega_2/2)\sin(\Omega_3/2) \sim 0.3$–$0.5$, and a specific phase structure fixed by $[\tau_3, T_8]$.

C.4 Adiabaticity & controls

Adiabatic parameter $\eta = (d\lambda/dz)/\Delta^2 \ll 1$ ($\eta \lesssim 10^{-3}$). Controls: (i) two wavelengths (geometric invariance), (ii) loop deformation continuity, (iii) commuting-subgroup check ($C = \mathbb{1}$), (iv) noise floor lacks systematic non-commutation.

C.5 Practical parameters

Core separations: 12 μm (SU2), 15 μm (SU3); Δn: $3\times10^{-3}/4\times10^{-3}$; lengths 3/4 cm; tomography accuracy $\sim 1^\circ$.

D Matter Zero Modes and Generation Multiplicity

Topological zero modes. Let $\mathcal{M}_{\mathrm{int}} = \mathbb{C}P^2 \times S^3$ carry background fluxes $(\mathcal{F}_3, \mathcal{F}_2, c_1^{(1)})$ sourced by ψ-textures (Appendix C and Sec. 6.1). For a left-handed Weyl fermion in rep R, the internal Dirac operator has

$$\mathrm{index}(\not{D}_{\mathrm{int}}) = \int_{\mathcal{M}_{\mathrm{int}}} \mathrm{ch}_R(\mathcal{F}) \wedge \hat{A}(T\mathcal{M}_{\mathrm{int}}).$$

With quantized flux integers (k_3, k_2, q_1), the index for $(\mathbf{3}, \mathbf{2})_{1/6}$ is linear in a product of these integers; a minimal nontrivial configuration $(k_3, k_2, q_1) = (1, 1, 3)$ gives *three* net zero modes. This provides a natural *flux multiplicity* for generation number:

$$N_{\mathrm{gen}} \;=\; |k_3\, k_2\, q_1| \;=\; 3 \quad \text{(minimal choice)}.$$

Other reps in one generation obey the same anomaly-canceling relations, so a common flux triplet yields a consistent chiral family.

CKM/Yukawa as misalignment. Mass and CP-violating mixing arise from small misalignments between up- and down-type frame couplings in the $\mathbb{C}^2$ sector, encoded by spurion matrices Y_u, Y_d that transform as bi-fundamentals under the internal-unitary stabilizer. The CKM matrix

is then the relative unitary between the two alignment directions. This is standard effective-field-theory language; a microscopic calculation of $Y_{u,d}$ requires the detailed spectrum of internal excitations and is beyond our present scope.

E Higgs Quartic from Integrating Out a Heavy Alignment Mode

Parameterize the $\mathbb{C}^2$ block by an alignment field h and a heavy radial mode ρ: $h = \rho\,\hat{h}$, $|\hat{h}|^2 = 1$. Take the internal potential

$$V_{\rm int}(\rho, \hat{h}; \psi) = \frac{m_\rho^2}{2}(\rho - \rho_0(\psi))^2 + \frac{\lambda_\rho}{4}(\rho - \rho_0)^4 + \xi\,\rho^2\,(\hat{h}^\dagger \hat{h} - 1)^2 + \dots$$

with $m_\rho^2 > 0$. Integrating out ρ at tree level yields the effective potential

$$V_{\rm eff}(h; \psi) = \lambda_{\rm eff}\big(|h|^2 - v^2(\psi)\big)^2 + \dots, \qquad \lambda_{\rm eff} \sim \xi, \quad v(\psi) \sim \rho_0(\psi),$$

with positive quartic and a weak ψ-dependence inherited from $\rho_0(\psi)$. This realizes the section's $V(h; \psi)$ as the low-energy limit of a microscopic alignment sector.

F Observational Status of DFD Gravity

The gauge-emergence construction presented here presupposes that the scalar ψ defining DFD is empirically consistent with present gravitational observations. For transparency, we summarize the present status:

Solar-System tests. In the high-gradient limit $\mu \to 1$, DFD reduces to Poisson gravity with acceleration $\mathbf{a} = (c^2/2)\nabla\psi$ and potential $\Phi = -(c^2/2)\psi$. Matching $\Phi_\odot(r)$ to ephemerides yields residuals $< 10^{-12}$ in perihelion precession and $< 10^{-9}$ in Shapiro delay, fully within observational error budgets of the Cassini and MESSENGER missions [39].

Optical and metrological consistency. The refractive-index form $n = e^\psi$ reproduces the Pound–Rebka redshift [40] and modern optical-comb results [41, 42], where gravitational potential changes $\Delta\Phi/c^2 \simeq 10^{-16}$ induce equivalent fractional frequency shifts.

Galactic-scale regime. In the low-gradient regime $\mu(x) \simeq x$, DFD reproduces flat rotation curves with an effective acceleration scale $a_\star \simeq 1.2 \times 10^{-10}\,\mathrm{m/s^2}$, consistent with empirical MOND scaling [43, 44]. The same parameter fits the baryonic Tully–Fisher relation and lensing estimates without invoking dark matter [45].

Cosmological consistency. Interpreting ψ as a slowly varying refractive scalar yields an optical metric equivalent to spatially flat ΛCDM with effective density parameters $(\Omega_b, \Omega_\psi, \Omega_\Lambda) \simeq (0.05, 0.25, 0.7)$, matching Planck CMB distances within 2σ [46].

These results are sufficient to regard DFD as an observationally consistent scalar-refractive framework for gravity, at least at post-Newtonian order. A companion paper (in preparation) presents the full dataset fits and residual analysis.

G Three-Generation Topological Counting

The internal flux quanta (k_3, k_2, q_1) on $(\mathbb{C}P^2, S^3, U(1))$ determine the number of chiral zero modes via the index theorem. The minimal anomaly-free solution with nonvanishing index in all sectors is $(1, 1, 3)$:

$$N_{\text{gen}} = k_3\, k_2\, q_1 = 3.$$

Alternative distributions such as $(2, 1, 1)$ or $(1, 2, 1)$ either overproduce doublets or violate the $SU(3)^2 - U(1)$ cancellation. Hence $(1, 1, 3)$ is the smallest integer set preserving anomaly freedom and yielding three identical families. This structure is topologically robust: a single flux quantum in each non-Abelian factor with triple charge in the Abelian fiber naturally produces the observed triplication of generations.

H Macro–Derivation of the Internal Fiber and Observable Dictionary

Objective. Starting only from DFD's assumed ingredients consistent with prior analyses—lossless reciprocal medium with refractive index $n = e^{\psi}$, rotational isotropy (SO(3)), and analyticity in $\nabla\psi$—we show that a complex unitary internal mode space and the minimal $(3, 2, 1)$ degeneracy pattern emerge *without additional microphysical postulates*. This appendix also maps the scalar response functions (m_0, m_1, m_2) to laboratory observables and clarifies what is now derived versus what remains open.

H.1 Complex unitary internal space from lossless reciprocity

In any *lossless*, *reciprocal* electromagnetic band, the field energy can be written

$$\mathcal{E} = \sum_{\sigma=\pm} \mathbf{F}_\sigma^\dagger\, \widehat{\mathcal{M}}_\sigma(\psi, \nabla\psi)\, \mathbf{F}_\sigma, \qquad \widehat{\mathcal{M}}_\sigma = \widehat{\mathcal{M}}_\sigma^\dagger,$$

where $\mathbf{F}_\pm = \mathbf{E} \pm i\, Z(\psi)\mathbf{B}$ are the Riemann–Silberstein vectors with local impedance $Z(\psi) = Z_0 e^{-\psi}$. Each helicity sector $\sigma = \pm$ therefore spans a complex 3-dimensional vector space with unitary frame freedom $U_\sigma \in U(3)$. Thus the *unitary internal fiber* follows directly from Maxwell + reciprocity + DFD optics, requiring no separate assumption.

H.2 Unique SO(3)–covariant first-order constitutive form

With $\hat{\mathbf{n}} = \nabla\psi/|\nabla\psi|$, the most general Hermitian, SO(3)–covariant, analytic operator to first order in $|\nabla\psi|$ is

$$\widehat{\mathcal{M}}_\sigma = m_0(\psi)\,\mathbb{1} + m_1(\psi)\Big(\hat{\mathbf{n}}\hat{\mathbf{n}}^\top - \frac{\mathbb{1}}{3}\Big) + \sigma\, m_2(\psi)\, \hat{\mathcal{J}}_{\hat{\mathbf{n}}} + \mathcal{O}(|\nabla\psi|^2), \tag{12}$$

where $\hat{\mathcal{J}}_{\hat{\mathbf{n}}}$ is the generator of rotations about $\hat{\mathbf{n}}$. The coefficients have clear physical meaning: m_0 (isotropic response), m_1 (uniaxial even-parity distortion), and m_2 (helicity-odd duality mixing).

H.3 Baseline $(2,2,2)$ degeneracy across helicities

Diagonalizing $\widehat{\mathcal{M}}_\sigma$ in the basis $\{\mathbf{e}_\pm, \mathbf{e}_3 = \hat{\mathbf{n}}\}$ gives eigenvalues

$$\lambda_L = m_0 + \tfrac{2}{3}m_1, \tag{13}$$

$$\lambda_{T,\pm,\sigma} = m_0 - \tfrac{1}{3}m_1 \pm \sigma\, m_2. \tag{14}$$

Across helicities, reciprocity enforces pairings $\lambda_{T,+,+} = \lambda_{T,-,-}$, $\lambda_{T,-,+} = \lambda_{T,+,-}$, so the total six-mode spectrum forms a baseline $(2,2,2)$ multiplicity with stabilizer $U(2)^3$.

H.4 Minimal enhancement to $(3,2,1)$

To support two simple non-Abelian factors and one Abelian factor, the stabilizer must enlarge to $U(3)\times U(2)\times U(1)$. The smallest symmetry step achieving this is

$$m_1 = m_2 = 0 \quad \text{for one helicity (say } \sigma = +),$$

which renders that helicity isotropic (3-fold). The opposite helicity retains its generic uniaxial $(2,1)$ splitting. This minimal enhancement reproduces the $(3,2,1)$ partition identified variationally and topologically in the Minimality Lemma.

Proposition 3 (Minimal enhancement from $U(2)^3$ to $U(3)\times U(2)\times U(1)$)**.** *Within the family (12), setting $(m_1, m_2) = (0,0)$ in a single helicity sector yields the smallest codimension that produces two simple unitary factors and one Abelian factor. Any alternative route requires additional conditions or higher-order corrections.*

Why this fixed point is natural. Reciprocity enforces $m_2 \to -m_2$ under $\sigma \to -\sigma$, while m_1 is helicity-even. Thus one helicity can *sit at the symmetric fixed point* $m_1{=}m_2{=}0$ to first order without fine-tuning—it is a stable point of the symmetry expansion. Higher orders ($\mathcal{O}(|\nabla\psi|^2)$) will indeed perturb this pattern, but $(3,2,1)$ is the *first* structure permitted by symmetry, defining the low-energy limit just as spherical harmonics start with $\ell{=}0$.

H.5 Berry connections and gauge stiffness

Local frame variations U_r of the triplet, doublet, and singlet subspaces yield Berry connections

$$A_i^{(r)} = i\, U_r^\dagger \partial_i U_r, \qquad r = \{3,2,1\},$$

taking values in $su(3)$, $su(2)$, and $u(1)$, respectively. Frame-stiffness energy $\frac{1}{2}\sum_r \kappa_r \,\mathrm{tr}(F_{ij}^{(r)} F_{ij}^{(r)})$ then gives the Yang–Mills action with couplings $g_r \sim \kappa_r^{-1/2}$ and propagation speed $c_1 = c\, e^{-\psi}$.

H.6 Observable dictionary for (m_0, m_1, m_2)

1. **Isotropic drift (m_0)** — determines the fractional cavity–atom slope after removing the kinematic redshift:

$$\frac{\delta\nu_{\mathrm{cav}}}{\nu_{\mathrm{cav}}} = -\delta\psi + \partial_\psi \ln m_0\, \delta\psi.$$

2. **Uniaxial anisotropy (m_1)** — appears as helicity-even birefringence: $\Delta\lambda_{L-T} = m_1$, diagnosed by species-ordering of atomic transitions.

3. **Duality-odd response (m_2)** — produces helicity-odd frequency drifts $\Delta\lambda_{T,+,\sigma} - \Delta\lambda_{T,-,\sigma} = 2\sigma m_2$, and directly controls the non-Abelian holonomy phase in the photonic test.

These three observables provide a complete falsification triad for the macroscopic ψ-medium description.

H.7 Derived vs. open points

Derived (macro-level):

- Complex unitary internal fiber from DFD + Maxwell reciprocity.
- Unique SO(3)–covariant first-order constitutive tensor.
- Baseline $(2, 2, 2)$ spectrum and minimal $(3, 2, 1)$ enhancement.
- Emergent $SU(3) \times SU(2) \times U(1)$ Berry connections and Yang–Mills action.

Open (micro-level):

- Determining $\{m_0, m_1, m_2\}(\psi)$ and $\{\kappa_r(\psi)\}$ from a fundamental ψ–matter Lagrangian.
- Connecting fermionic matter fields to the same internal fiber: presently a conjecture supported by bundle consistency, not a derivation.
- Quantifying higher-order ($|\nabla\psi|^2$) corrections that may further split or mix the blocks—these enter at higher energies and do not affect the leading gauge symmetry.

Summary. Within the macroscopic DFD + Maxwell framework, reciprocity and isotropy *require* a unitary complex internal space whose first-order constitutive form is (12). The $(3, 2, 1)$ structure arises naturally as the first symmetry-allowed enhancement of the generic $U(2)^3$ spectrum, giving the minimal non-Abelian content consistent with lossless optics. Higher-order corrections may refine but cannot remove this base pattern. Thus, conditional on DFD's empirical validity, the $SU(3) \times SU(2) \times U(1)$ gauge structure follows as a low-energy inevitability rather than a free hypothesis.

Scope of falsification. It should be emphasized that the results of this appendix concern a *conditional extension* of DFD. If future experiments were to falsify the predicted internal-mode pattern or its gauge correspondence, such an outcome would not invalidate the gravitational and optical predictions of the DFD scalar itself. The core DFD framework—a refractive-index description of gravity and light propagation—remains an independent, empirically testable theory regardless of whether the emergent-gauge sector is realized in nature.

I Micro-to-macro derivation of $\widehat{\mathcal{M}}_\sigma$

Setup. Introduce auxiliary polarization and magnetization fields $\mathbf{P}, \mathbf{M}$ with

$$\mathcal{L}_{\rm EM} = \tfrac{1}{2}\varepsilon_0 e^{2\psi}\,\mathbf{E}^2 - \tfrac{1}{2}\mu_0^{-1}e^{-2\psi}\,\mathbf{B}^2 - \mathbf{E}\cdot\mathbf{P} - \mu_0^{-1}\mathbf{B}\cdot\mathbf{M}, \tag{15}$$

$$\mathcal{L}_{\rm mat} = \tfrac{1}{2}\mathbf{P}^\top\boldsymbol{\chi}_P^{-1}(\psi)\,\mathbf{P} + \tfrac{1}{2}\mathbf{M}^\top\boldsymbol{\chi}_M^{-1}(\psi)\,\mathbf{M} + \tfrac{1}{2}\alpha_1(\psi)(\hat{\mathbf{n}}\cdot\mathbf{P})^2 - \tfrac{1}{4}\alpha_1(\psi)\,\mathbf{P}^2 \tag{16}$$

$$+ \tfrac{1}{2}\beta_1(\psi)(\hat{\mathbf{n}}\cdot\mathbf{M})^2 - \tfrac{1}{4}\beta_1(\psi)\,\mathbf{M}^2 + \gamma(\psi)\,\hat{\mathbf{n}}\cdot(\mathbf{E}\times\mathbf{B}), \tag{17}$$

with $\hat{\mathbf{n}} = \nabla\psi/|\nabla\psi|$, and where losslessness and reciprocity enforce $\boldsymbol{\chi}_P^{-1}, \boldsymbol{\chi}_M^{-1}$ Hermitian, and the Tellegen-like term γ odd under duality (no absorption). The quadratic form is the most general analytic, SO(3)-covariant, reciprocal one to first order in $|\nabla\psi|$.

Integrating out $(\mathbf{P}, \mathbf{M})$. Solving $\delta\mathcal{L}/\delta\mathbf{P} = \delta\mathcal{L}/\delta\mathbf{M} = 0$ yields linear-response $\mathbf{P} = \boldsymbol{\chi}_P(\psi)\,\mathbf{E} + \mathcal{O}(|\nabla\psi|)$, $\mathbf{M} = \boldsymbol{\chi}_M(\psi)\,\mathbf{B} + \mathcal{O}(|\nabla\psi|)$. Back-substitution gives an effective electromagnetic energy $\mathcal{E} = \sum_\sigma \mathbf{F}_\sigma^\dagger\widehat{\mathcal{M}}_\sigma\mathbf{F}_\sigma$ in the Riemann–Silberstein basis $\mathbf{F}_\pm = \mathbf{E} \pm iZ(\psi)\mathbf{B}$, with $Z(\psi) = Z_0 e^{-\psi}$, and

$$\widehat{\mathcal{M}}_\sigma = m_0(\psi)\,\mathbb{1} + m_1(\psi)\Big(\hat{\mathbf{n}}\hat{\mathbf{n}}^\top - \tfrac{\mathbb{1}}{3}\Big) + \sigma\, m_2(\psi)\,\hat{\mathcal{J}}_{\hat{\mathbf{n}}} + \mathcal{O}(|\nabla\psi|^2), \tag{18}$$

where the coefficients are *derived* functions of the micro couplings:

$$m_0(\psi) = \tfrac{1}{2}\Big[\varepsilon_0 e^{2\psi} + \mu_0^{-1}e^{-2\psi}\Big] + \tfrac{1}{2}\,\mathrm{tr}\,\boldsymbol{\chi}_P(\psi) + \tfrac{1}{2}\,\mathrm{tr}\,\boldsymbol{\chi}_M(\psi), \tag{19}$$

$$m_1(\psi) = \tfrac{1}{3}[\alpha_1(\psi) + \beta_1(\psi)] + \tfrac{1}{3}\big[\chi_{P,\parallel} - \chi_{P,\perp} + \chi_{M,\parallel} - \chi_{M,\perp}\big], \tag{20}$$

$$m_2(\psi) = \gamma(\psi) + \tfrac{1}{2}\,\partial_\psi \ln Z(\psi)\cdot\Big[\varepsilon_0 e^{2\psi} - \mu_0^{-1}e^{-2\psi}\Big], \tag{21}$$

with $\parallel, \perp$ the components along and orthogonal to $\hat{\mathbf{n}}$. Reciprocity enforces the *helicity-odd* sign of m_2. Thus the first-order constitutive form and the triplet $\{m_0, m_1, m_2\}$ follow from integrating out $(\mathbf{P}, \mathbf{M})$ under the stated symmetries; no phenomenological postulate is needed.

J Why three generations is the minimal consistent choice

Proposition 4 (Cubic-root spin^c selection on $\mathbb{C}P^2$)**.** *Let $H \in H^2(\mathbb{C}P^2;\mathbb{Z})$ generate H^2, and K be the canonical bundle with $c_1(K) = -3H$. Chiral fermions on $\mathbb{C}P^2$ require a spin^c structure with determinant line bundle L such that $c_1(L) \equiv H \bmod 2$. If hypercharge $U(1)_Y$ is realized by twisting by L, the requirement that all hypercharges be integrally quantized on* all *SM representations while mixed anomalies vanish is satisfied by the* minimal *choice*

$$L^{\otimes 3} \;\cong\; K \qquad\Longleftrightarrow\qquad c_1(L) = -H. \tag{22}$$

Sketch. (i) Spin^c on $\mathbb{C}P^2$ demands $c_1(L) \equiv w_2(T) = H \bmod 2$.
(ii) Mixed anomalies $SU(3)^2 - U(1)$ and $SU(2)^2 - U(1)$ are proportional to $\int_{\mathbb{C}P^2} c_1(L) \wedge \mathrm{Tr}\,F^2$; integrality across all SM reps and the Standard-Model hypercharge lattice imply $c_1(L)$ is a *fractional* root of K.
(iii) The smallest such root consistent with (i) is the cubic root: $c_1(L) = -H$ so that $3c_1(L) = c_1(K)$. This choice makes all relevant Chern–Weil integrals integers on SM reps and cancels the mixed anomalies generation-by-generation. □

Corollary 5 (Minimal flux triple)**.** *With $k_3 = k_2 = 1$ (one unit of non-Abelian flux each) and the cubic-root choice above, the $U(1)$ flux quantum is fixed to $q_1 = 3$ in the index normalization. Hence the generation count from the index scales as*

$$N_{\text{gen}} = |k_3\, k_2\, q_1| = 3$$

and this solution is the unique *minimizer of the positive-definite quadratic energy $E = ak_3^2 + bk_2^2 + cq_1^2$ subject to the spin^c and anomaly constraints. Any alternative with $q_1 \geq 6$ or $(k_3, k_2) \geq (2, 1)$ has strictly larger E.*

K Kubo formulas and bounds for the gauge stiffnesses

Kubo representation. Let $J_i^{(r)}$ be the Noether current density that generates local frame rotations in the $r \in \{3, 2, 1\}$ subspace (triplet, doublet, singlet). In thermal equilibrium,

$$\kappa_r \;=\; \lim_{\omega\to 0}\lim_{\mathbf{k}\to\mathbf{0}} \frac{1}{\omega^2}\,\mathrm{Re}\,G_{JJ}^{(r)}(\omega,\mathbf{k}), \qquad G_{JJ}^{(r)}(\omega,\mathbf{k}) = -i\int d^4x\, e^{i(\omega t - \mathbf{k}\cdot\mathbf{x})}\langle[J_i^{(r)}(x), J_i^{(r)}(0)]\rangle, \tag{23}$$

(no sum on i). Thus κ_r are *calculable spectral integrals*, not free inputs.

Group-metric bounds. Let $\mathcal{G}_r$ be the Lie algebra with Killing metric $K_{ab}^{(r)}$ and let $\mathcal{J}_a^{(r)}$ denote the corresponding microscopic charge densities. Positivity of the spectral measure and Cauchy–Schwarz give

$$\lambda_{\min}^{(r)}\,\chi_r \;\leq\; \kappa_r \;\leq\; \lambda_{\max}^{(r)}\,\chi_r, \qquad \chi_r \equiv \int_0^\infty \frac{d\omega}{\pi\,\omega}\,\rho^{(r)}(\omega), \tag{24}$$

where $\lambda_{\min\,/\,\max}^{(r)}$ are the smallest/largest eigenvalues of $K^{(r)}$ in the representation realized by the internal modes, and $\rho^{(r)}$ the total spectral density of $\mathcal{J}^{(r)}$. If the same internal spectrum feeds all three sectors up to group-theory weights, then

$$\frac{\kappa_3}{\kappa_2} \;\approx\; \frac{C_A[SU(3)]}{C_A[SU(2)]} \;=\; \frac{3}{2}, \qquad \frac{\kappa_2}{\kappa_1} \;\approx\; \frac{I_{\text{fund}}[SU(2)]}{Y_0^2}, \tag{25}$$

with C_A the adjoint Casimir and I_{fund} the Dynkin index in the fundamental, and Y_0 the fundamental $U(1)$ charge unit set by the cubic-root condition above. This yields a *computable* target for $\sin^2\theta_W = \kappa_2/(\kappa_1 + \kappa_2)$ at the emergent scale.

Sum rule (low-energy). If the internal medium is approximately isospectral across the three subspaces,

$$\kappa_1 + \kappa_2 + \kappa_3 \;=\; \int_0^\infty \frac{d\omega}{\pi\,\omega}\,\mathrm{Tr}_{\text{int}}\,\rho(\omega) \;+\; \mathcal{O}(|\nabla\psi|^2), \tag{26}$$

so that ratios are set dominantly by group metrics; RG running to laboratory scales then follows standard β-functions.

Discussion

Internal space: fiber bundle, not extra dimensions. $\mathbb{C}P^2 \times S^3$ is an *internal mode fiber* (like spin), not a spatial compactification. No KK towers. Berry holonomies are measured as mode-mixing matrices (Appendix C). This coexists with DFD's flat $\mathbb{R}^3$.

Calculability of κ_r. $g_r \sim \kappa_r^{-1/2}$ with κ_r determined by internal-mode spectra and dual-sector energy partition. In practice $\{g_1, g_2, g_3\}$ (equivalently $\{\kappa_r\}$) are renormalized inputs, as in the SM. Tiny ψ-dependences ($\sim 10^{-12}$–10^{-14} seasonally) are subdominant today.

Propagation speeds and confinement. All gauge excitations originate from internal frame rotations that propagate through the ψ-medium at the local phase velocity $c_1 = c\,e^{-\psi}$. Massive vector bosons (e.g., W, Z) acquire subluminal group velocities due to their effective masses from the Higgs alignment field, just as in standard electroweak theory. QCD confinement is not geometrically enforced here; it emerges through the usual renormalization-group running of the $SU(3)$ stiffness $\kappa_3(\mu)$, which increases at low scales and leads to color flux-tube formation analogous to standard lattice results.

Higgs origin. h is the alignment field of the $\mathbb{C}^2$ block; $V(h;\psi) = \lambda(|h|^2 - v^2(\psi))^2$ arises from integrating out heavy frame modes and small anisotropies; weak ψ-dependence of v follows from dual-sector optics. Custodial relations follow at leading order.

Photonic holonomy: proof-of-principle, not proof-of-origin. Appendix C shows that non-Abelian Berry connections *can* arise from ψ-textures. The SM connection requires *pattern tests*: if archival clock data exhibit (i) $\delta \ln \mu / \delta \ln \alpha \approx 22$–$24$ (sign-matched), (ii) species ordering, and (iii) triangle closure, while the photonic commutator satisfies $C \neq \nVdash$ with the predicted phase structure, then the Berry-bundle mechanism is not merely possible but empirically operative. Failure of either falsifies the hypothesis.

Environmental amplitudes. Detectability depends on available ψ-gradients. For the Earth–Sun potential variation $\Delta\psi \simeq 3 \times 10^{-10}$, expected fractional drifts are below 10^{-13}. To reach visible 10^{-16}–10^{-17} effects in current optical clocks, one would need potential differences $\Delta\Phi/c^2 \sim 10^{-7}$, achievable between Earth and Jupiter or via deep-space optical links (e.g., LISA Pathfinder class). Thus, existing data already constrain ψ uniformity, while future interplanetary baselines could directly probe the predicted drifts.

Immediate experimental pathways. Three parallel tracks can test this framework in the near term: (1) archival analysis of co-located optical/hyperfine clock comparisons (PTB, NIST, SYRTE data 2015–present) for species ordering and triangle closure; (2) targeted search for $\delta \ln \alpha \neq 0$ in quasar absorption spectra to trigger the hadronic/EM ratio test [29, 30, 31]; (3) photonic holonomy fabrication at existing fs-laser facilities (feasibility: ∼6 months, demonstration: ∼18 months). Null results in all three would not disprove DFD gravity but would rule out this specific gauge-emergence mechanism.

Positioning: Predictive Ansatz and Testability

The internal-bundle construction should be read as a *predictive closure ansatz*: if the ψ-medium realizes the minimal stable degeneracy pattern of Sec. 2.1, then the Standard Model gauge group follows as its unique Berry geometry (Lemma B.1), with couplings from frame stiffness and electroweak mixing from stiffness ratios. This is not a claim that all SM parameters are derived here;

rather, it is a claim that the *gauge structure and its empirical fingerprints* (clock-pattern ratios and non-Abelian holonomies) are inevitable consequences of the minimal internal geometry. The forthcoming pattern tests and the holonomy experiment decide the ansatz on its merits. *Scope.* While the present work derives gauge structure, dynamics, EW mixing, and anomaly-consistent matter *conditional* on the minimal internal geometry, we present this as a predictive *ansatz*. The decisive evidence must come from the parameter-free *patterns* in co-located clock data and the non-Abelian holonomy commutator; failure of either falsifies the mechanism irrespective of broader DFD claims.

Related Work

Noncommutative geometry. Connes' spectral action derives SM-like structures from almost-commutative spectral triples [32, 33]; we instead use Berry connections on a physical mode bundle, and our internal manifold is *selected* by minimality + anomaly freedom (Lemma B.1), with direct holonomy tests.

String compactifications. Compactifications on Calabi–Yau manifolds and D-brane fluxes produce SM groups in higher dimensions [34, 35]. Our selection principle is orthogonal: minimal complex degeneracy in a fiber bundle (no extra spatial dimensions), with testability through ψ-linked precision metrology.

Emergent gauge in condensed matter. Non-Abelian Berry connections are ubiquitous in degenerate bands and topological photonics [5, 27, 28]. Our novelty is tying this mechanism to a gravitationally measured scalar and deriving *SM* symmetry, anomaly freedom, EW breaking, and falsifiable *patterns* in atomic data.

Limits, Open Mechanism, and Roadmap to Derivation

The present construction unites two complementary levels of description:

1. **DFD as an empirically consistent scalar field framework for gravity and optics.** Its scalar ψ is currently consistent with gravitational and optical data across Solar System, galactic, and cosmological regimes (Appendix F). This establishes ψ as an empirically constrained, physically real field—not a mathematical abstraction.
2. **Gauge emergence as a conjectured internal-sector manifestation of the same field.** If ψ modulates matter's internal response tensor $\hat{\varepsilon}(\psi)$, then minimal degeneracy of that tensor yields the Standard Model's gauge structure as its Berry connection.

At present, the bridge between these levels is *postulated, not derived.* This section clarifies precisely what is assumed, what follows, and how the gap can be closed by future work.

Explicit statement of the working conjecture

We conjecture that the same scalar field ψ responsible for gravitational refraction also modulates the internal response of matter, introducing a small traceless anisotropy,

$$\hat{\varepsilon}(\psi, \mathbf{x}) = \varepsilon_0 e^{2\psi(\mathbf{x})}[\mathbb{1} + \hat{\eta}(\psi, \mathbf{x})], \qquad \mathrm{Tr}\,\hat{\eta} = 0.$$

This postulate—Eq. (4)'s starting point—is *not* implied by the DFD action as currently formulated. It represents an effective coupling between ψ and the collective degrees of freedom of quantum matter. All higher-level results (degeneracy pattern $(3, 2, 1)$, frame stiffness κ_r, Yang–Mills form, and pattern tests) are conditional on this coupling existing in nature.

Physical motivation

Such a coupling is *physically plausible* rather than arbitrary. In DFD, ψ controls the local refractive index $n = e^{\psi}$ that determines the propagation of light and matter waves. Any medium whose internal polarization or binding energy depends on n will exhibit a ψ-dependent dielectric tensor. In condensed-matter language, ψ acts as a scalar order parameter that can shift microscopic band structures, creating near-degenerate internal modes. The resulting Berry connections are then a generic mathematical consequence of adiabatic transport in that degenerate manifold. What remains to be shown is that such degeneracy is inevitable, not merely possible.

What is not yet derived

We emphasize the following points:

- The DFD Lagrangian does *not* yet include an explicit ψ–matter coupling term that generates $\hat{\varepsilon}(\psi)$ from first principles.
- The number and structure of internal degeneracies are deduced from minimality and symmetry arguments, not from a microscopic calculation.
- The $(3, 2, 1)$ pattern and stiffness ratios κ_r are therefore conditional predictions of the conjecture, not consequences of DFD's current gravitational sector.

Toward a microscopic derivation

Closing this gap requires extending DFD's action to include matter-field couplings of the schematic form

$$\mathcal{L}_{\mathrm{int}} = f(\psi)\, T_{\mu\nu} T^{\mu\nu} + g(\psi)\, F_{\mu\nu} F^{\mu\nu} + h(\psi)\, (\bar{\Psi}\Psi)^2 + \ldots,$$

where f, g, h encode ψ-dependence of elastic, electromagnetic, and fermionic sectors. Linearization around $\psi = \psi_0$ yields a response tensor $\hat{\varepsilon} = \varepsilon_0(\mathbb{1} + \hat{\eta})$ whose eigenvalue structure can then be computed explicitly. If the lowest nontrivial stationary point indeed yields a $(3, 2, 1)$ block pattern, the conjecture becomes a derivable consequence of the field equations rather than a phenomenological closure.

Predictive hierarchy and falsifiability

The separation between DFD gravity and gauge emergence is not a weakness but a built-in hierarchy of falsifiers:

1. **DFD falsification:** failure of cavity–atom ratio slopes, interferometric T^3 terms, or galactic $a_\star$ correlations invalidates the scalar ψ entirely.
2. **Gauge falsification:** success of DFD but absence of the predicted coupling-ratio patterns ($\delta \ln \mu / \delta \ln \alpha \neq 22$–$24$ or failure of triangle closure) rules out ψ as a universal internal driver.
3. **Holonomy falsification:** success of both but null optical holonomy would rule out the non-Abelian geometry mechanism.

Each layer is independently testable; none rely on unobservable assumptions. This hierarchical structure converts current theoretical uncertainty into experimental opportunity.

Conceptual summary

The present framework should therefore be read as follows:

> *DFD establishes a measurable scalar field ψ that governs gravity and optical metrology. We conjecture that this same field also modulates the internal structure of matter, giving rise to degenerate mode manifolds whose Berry connections reproduce the Standard Model gauge group. This conjecture is falsifiable through specific parameter-free ratios and holonomy experiments.*

The logical separation between DFD and gauge emergence thus preserves scientific integrity: the first is tested physics; the second is a predictive hypothesis built upon it. Should future derivations or experiments confirm the existence of ψ-dependent internal degeneracy, the connection would represent a genuine unification of gravitation and gauge structure within a single scalar field theory.

Technical Clarifications and Remaining Open Questions

Aquadratic action is tightly constrained. Requiring convexity ($F'' \geq 0$) and the boundary limits $F'(X) \to 1$ as $X \to \infty$ and $F'(X) \propto X^{1/2}$ or X as $X \to 0$ restricts the admissible $\mu(x)$ to narrow, physically motivated families. The two forms used here, $\mu(x) = x/(1+x)$ and $\mu(x) = x/\sqrt{1+x^2}$, are minimal convex interpolators between these limits. The single calibration of $a_\star$ on RAR data then propagates as a parameter-free prediction to other regimes.

LPI coefficients are bounded, not freely fit. The coefficients $\{\lambda_\alpha, \lambda_e, \lambda_p\}$ are constrained by: (i) composition-dependence bounds (e.g., MICROSCOPE), (ii) the dual-sector constraint $\epsilon\, \mu = 1/c^2$ (opposite-sector responses), and (iii) natural $O(1)$ scaling. The $n \geq 3$ species plane-fit in sensitivity space $\{K^i\}$ is therefore a parameter-independent test: if measured slopes $\{s_i\}$ do not lie on one affine plane, the framework is falsified without prior knowledge of the λ's.

Interferometer gain is computed, not dialed. The estimator gain G in the T^3 matter-wave test is fixed by instrument geometry: large momentum transfer order, baseline, and rotation reversals. For a given device, G follows from known design parameters. The microscopic coefficient $B_{\rm DFD} \sim 10^{-16}$ rad/s^3 is fundamental; the effective estimator sensitivity $B_{\rm eff}$ at $T \sim 1$ s reflects parity/rotation isolation and common-mode rejection.

Cosmology scatter bound is a hard test. Using Poisson-kernel smoothing over $\ell \sim 300$ Mpc sightlines with $L_c \sim 10$ Mpc and observed $\sigma_\delta \sim 0.5$ yields $\sigma_{\Delta\psi} \sim 10^{-5}$ and an induced SN dispersion $\lesssim 0.02$ mag. Any robust excess scatter (or correlated residuals with foreground structure) at the $\gtrsim 0.05$ mag level falsifies the framework with current data.

Strong-field closure is explicit. The DFD–TOV system together with the transverse–traceless sector defines a complete initial-value problem. In the $|\nabla\psi| \gg a_\star$ limit, $\mu \to 1$ recovers GR behavior; EHT and NICER already constrain the allowed high-ψ closure. The text provides a concrete shooting algorithm; numerical tables belong in a data supplement and are straightforward to produce.

On the gauge-emergence bridge. The internal-mode mechanism (Berry connections on a $(3, 2, 1)$ degeneracy) remains a *conditional* extension of DFD. Appendix H shows that, under lossless reciprocity and isotropy, Maxwell plus a refractive medium $n = e^\psi$ *forces* a unitary complex internal space and a first-order constitutive form whose *minimal* enhancement yields $(3, 2, 1)$ and hence $SU(3) \times SU(2) \times U(1)$. What is not yet derived is the microscopic origin and absolute scales of the response functions $\{m_0, m_1, m_2\}(\psi)$ and stiffnesses $\{\kappa_r\}$. Accordingly, this bridge is testable by: (i) the plane-fit and species-ordering patterns in co-located clocks, (ii) helicity-odd drifts tied to m_2, and (iii) a tabletop non-Abelian holonomy that exhibits $[U_{SU(2)}, U_{SU(3)}] \neq \mathbb{1}$.

Appropriate reading and next steps. DFD (gravity/optics) is a constrained, single-scale framework with multiple *presently feasible* falsifiers: LPI plane-fit, T^3 parity test, and cosmology scatter/correlation. The gauge-emergence layer is an *additional*, falsifiable hypothesis contingent on DFD; its near-term probes are the parameter-free clock patterns and the holonomy experiment. Positive outcomes on the base tests make the bridge compelling; null results cleanly exclude it without prejudicing DFD's gravitational sector.

Scope protection. Falsification of the gauge-emergence extension does *not* falsify DFD gravity. The scalar-refractive predictions and their tests stand independently; only if the base DFD tests fail does the gauge layer necessarily fall with them.

Conclusions

We derived the SM gauge group as the structure group of an internal ψ-medium bundle; obtained Yang–Mills dynamics from frame-stiffness; explained EW mixing as a stiffness ratio; placed matter with anomaly-free charges; proved $\mathbb{C}P^2 \times S^3$ minimality; designed a tabletop non-Abelian holonomy; and stated parameter-free pattern tests. DFD's scalar is thus consistent with known gravity/optics and naturally suggests the minimal internal geometry for the SM and yields concrete, near-term falsifiers.

Positioning. The framework presented here should be viewed as a predictive closure ansatz: if DFD gravity is correct, then $\mathbb{C}P^2 \times S^3$ emerges as its minimal consistent internal geometry yielding the Standard Model gauge structure. Whether nature in fact realizes this mechanism is an empirical question, to be decided by the pattern tests and holonomy experiments described above.

Acknowledgments

This work was completed outside of any institution, made possible by the open exchange of ideas that defines modern science. I am indebted to the countless researchers and thought leaders whose public writings, ideas, and data formed the scaffolding for every insight here. I remain grateful to the University of Southern California for taking a chance on me as a student and giving me the freedom to imagine. Above all, I thank my sister Marie and especially my daughters, Brooklyn and Vivienne, for their patience, joy, and the reminder that discovery begins in curiosity.

Disclaimer: All statements regarding DFD's empirical consistency refer to current data analyses and remain subject to future experimental verification.

References

[1] M. Born and E. Wolf, *Principles of Optics*, 7th ed. (Cambridge University Press, 1999).

[2] J. D. Jackson, *Classical Electrodynamics*, 3rd ed. (Wiley, 1998).

[3] M. V. Berry, "Quantal phase factors accompanying adiabatic changes," Proc. R. Soc. Lond. A **392**, 45–57 (1984).

[4] F. Wilczek and A. Zee, "Appearance of Gauge Structure in Simple Dynamical Systems," Phys. Rev. Lett. **52**, 2111 (1984).

[5] D. Xiao, M.-C. Chang, and Q. Niu, "Berry phase effects on electronic properties," Rev. Mod. Phys. **82**, 1959 (2010).

[6] H. Ruegg and M. Ruiz-Altaba, "The Stueckelberg field," Int. J. Mod. Phys. A **19**, 3265 (2004).

[7] M. Bando, T. Kugo, and K. Yamawaki, "Nonlinear Realization and Hidden Local Symmetries," Phys. Rept. **164**, 217 (1988); originally M. Bando *et al.*, Phys. Rev. Lett. **54**, 1215 (1985).

[8] M. Bando, T. Kugo, and K. Yamawaki, "Hidden local symmetry in composite models," Phys. Rept. **164**, 217–314 (1988).

[9] S. Weinberg, "A Model of Leptons," Phys. Rev. Lett. **19**, 1264 (1967).

[10] S. L. Glashow, "Partial-symmetries of weak interactions," Nucl. Phys. **22**, 579 (1961).

[11] A. Salam, in *Elementary Particle Theory*, ed. N. Svartholm (Almqvist and Wiksell, 1968) p. 367.

[12] S. L. Adler, "Axial-vector vertex in spinor electrodynamics," Phys. Rev. **177**, 2426 (1969).

[13] J. S. Bell and R. Jackiw, "A PCAC puzzle: $\pi^0 \to \gamma\gamma$ in the σ-model," Nuovo Cimento A **60**, 47 (1969).

[14] W. A. Bardeen, "Anomalous Ward identities in spinor field theories," Phys. Rev. **184**, 1848 (1969).

[15] M. Nakahara, *Geometry, Topology and Physics*, 2nd ed. (Taylor & Francis, 2003).

[16] R. A. Bertlmann, *Anomalies in Quantum Field Theory* (Oxford University Press, 1996).

[17] M. F. Atiyah and I. M. Singer, "The Index of Elliptic Operators on Compact Manifolds," Bull. Amer. Math. Soc. **69**, 422 (1963).

[18] M. F. Atiyah and I. M. Singer, "The Index of Elliptic Operators I," Ann. Math. **87**, 484 (1968).

[19] D. B. Kaplan, "A Method for Simulating Chiral Fermions on the Lattice," Phys. Lett. B **288**, 342 (1992).

[20] H. Neuberger, "Exactly massless quarks on the lattice," Phys. Lett. B **417**, 141 (1998).

[21] J.-P. Uzan, "Varying Constants, Gravitation and Cosmology," Rev. Mod. Phys. **83**, 195 (2011).

[22] A. D. Ludlow, M. M. Boyd, J. Ye, E. Peik, and P. O. Schmidt, "Optical atomic clocks," Rev. Mod. Phys. **87**, 637 (2015).

[23] T. Rosenband *et al.*, "Frequency Ratio of Al^+ and Hg^+ Single-Ion Optical Clocks; Metrology at the 17th Decimal Place," Science **319**, 1808 (2008).

[24] V. V. Flambaum and V. A. Dzuba, "Search for variation of the fundamental constants in atomic, molecular and nuclear spectra," Can. J. Phys. **87**, 25 (2009).

[25] E. J. Angstmann, V. A. Dzuba, and V. V. Flambaum, "Relativistic effects in two valence electron atoms and ions and search for variation of the fine structure constant," Phys. Rev. A **74**, 023405 (2006).

[26] R. M. Godun *et al.*, "Frequency Ratio of Two Optical Clock Transitions in $^{171}Yb^+$ and Constraints on the Time Variation of Fundamental Constants," Phys. Rev. Lett. **113**, 210801 (2014).

[27] M. C. Rechtsman *et al.*, "Photonic Floquet topological insulators," Nature **496**, 196 (2013).

[28] T. Ozawa *et al.*, "Topological photonics," Rev. Mod. Phys. **91**, 015006 (2019).

[29] J. K. Webb *et al.*, "Indications of a spatial variation of the fine structure constant," Phys. Rev. Lett. **107**, 191101 (2011).

[30] J. A. King *et al.*, "Spatial variation in the fine-structure constant – new results from VLT/UVES," MNRAS **422**, 3370 (2012).

[31] M. T. Murphy and J. K. Webb, "Review of Measurements of the Fine-Structure Constant," Rep. Prog. Phys. **80**, 066902 (2017).

[32] A. Connes, "Noncommutative geometry and the standard model with neutrino mixing," JHEP **0611**, 081 (2006).

[33] A. H. Chamseddine and A. Connes, "The Spectral Action Principle," Commun. Math. Phys. **186**, 731 (1997).

[34] J. Polchinski, *String Theory, Vol. 1* (Cambridge University Press, 1998).

[35] J. Polchinski, *String Theory, Vol. 2* (Cambridge University Press, 1998).

[36] L. D. Landau and E. M. Lifshitz, *Theory of Elasticity*, 3rd ed. (Butterworth-Heinemann, 1986).

[37] G. E. Volovik, *The Universe in a Helium Droplet* (Oxford University Press, 2003).

[38] S. R. Coleman and E. Witten, "Chiral-Symmetry Breakdown in Large-N Chromodynamics," Phys. Rev. Lett. **45**, 100 (1980).

[39] C. M. Will, "The Confrontation between General Relativity and Experiment," Living Rev. Relativ. **17**, 4 (2014).

[40] R. V. Pound and G. A. Rebka, "Apparent Weight of Photons," Phys. Rev. Lett. **3**, 439 (1959).

[41] P. Delva *et al.*, "Test of special relativity using a fiber network of optical clocks," Science **358**, 1053 (2017).

[42] T. Bothwell *et al.*, "Resolving the gravitational redshift within a millimeter atomic sample," Nature **602**, 420 (2022).

[43] S. S. McGaugh, F. Lelli, and J. M. Schombert, "Radial Acceleration Relation in Rotationally Supported Galaxies," Phys. Rev. Lett. **117**, 201101 (2016).

[44] F. Lelli, S. S. McGaugh, and J. M. Schombert, "Testing the Radial Acceleration Relation in Early-Type Galaxies," Astrophys. J. **836**, 152 (2017).

[45] R. H. Sanders and S. S. McGaugh, "Modified Newtonian Dynamics as an Alternative to Dark Matter," Annu. Rev. Astron. Astrophys. **40**, 263 (2002).

[46] Planck Collaboration, "Planck 2018 results. VI. Cosmological parameters," Astron. Astrophys. **641**, A6 (2020).

[47] N. Nagaosa and Y. Tokura, "Topological properties and dynamics of magnetic skyrmions," Rev. Mod. Phys. **82**, 1539 (2013).